PLOS PATHOGENS

RESEARCH ARTICLE

MAVS regulates the quality of the antibody response to West-Nile Virus

Marvin O'Ketch[1], Spencer Williams[1], Cameron Larson[1], Jennifer L. Uhrlaub[1], Rachel Wong[1,2], Brenna Hall[1], Neha R. Deshpande[1], Dominik Schenten[1]*

1 Department of Immunobiology, University of Arizona, Tucson, Arizona, United States of America, **2** Division of Biological and Biomedical Sciences, Washington University in St. Louis, Saint Louis, Missouri, United States of America

* dschenten@email.arizona.edu

Citation: O'Ketch M, Williams S, Larson C, Uhrlaub JL, Wong R, Hall B, et al. (2020) MAVS regulates the quality of the antibody response to West-Nile Virus. PLoS Pathog 16(10): e1009009. https://doi.org/10.1371/journal.ppat.1009009

Editor: Sonja Best, National Institute of Allergy and Infectious Diseases, UNITED STATES

Received: March 25, 2020

Accepted: September 28, 2020

Published: October 26, 2020

Data Availability Statement: All relevant data are within the manuscript and its Supporting Information files.

Funding: This work was supported by the National Institutes of Health through R56AI130044 and R21AI146388 and the Arizona Biomedical Research Foundation to D. S. The funders had no role in study design, data collection and analysis, decision to publish, or preparation of the manuscript.

Competing interests: The authors have declared that no competing interests exist.

Abstract

A key difference that distinguishes viral infections from protein immunizations is the recognition of viral nucleic acids by cytosolic pattern recognition receptors (PRRs). Insights into the functions of cytosolic PRRs such as the RNA-sensing Rig-I-like receptors (RLRs) in the instruction of adaptive immunity are therefore critical to understand protective immunity to infections. West Nile virus (WNV) infection of mice deficent of RLR-signaling adaptor MAVS results in a defective adaptive immune response. While this finding suggests a role for RLRs in the instruction of adaptive immunity to WNV, it is difficult to interpret due to the high WNV viremia, associated exessive antigen loads, and pathology in the absence of a MAVS-dependent innate immune response. To overcome these limitations, we have infected MAVS-deficient ($MAVS^{KO}$) mice with a single-round-of-infection mutant of West Nile virus. We show that $MAVS^{KO}$ mice failed to produce an effective neutralizing antibody response to WNV despite normal antibody titers against the viral WNV-E protein. This defect occurred independently of antigen loads or overt pathology. The specificity of the antibody response in infected $MAVS^{KO}$ mice remained unchanged and was still dominated by antibodies that bound the neutralizing lateral ridge (LR) epitope in the DIII domain of WNV-E. Instead, $MAVS^{KO}$ mice produced IgM antibodies, the dominant isotype controlling primary WNV infection, with lower affinity for the DIII domain. Our findings suggest that RLR-dependent signals are important for the quality of the humoral immune response to WNV.

Author summary

A key difference that distinguishes viral infection from protein immunization is the detection of viral nucleic acids by cytosolic pattern recognition receptors (PRRs) including the RNA-sensing Rig-I-like receptors (RLRs). Insights into the specific function of RLRs are therefore critical for the understanding of protective immunity to infections. Here, we have infected mice deficient in RLR signaling with an attenuated mutant of West Nile virus (WNV). We show that the anti-viral antibody response of these mice failed to neutralize the virus effectively because the majority of WNV-specific antibodies poorly bound

the virus. Our findings suggest that the detection of WNV by RLRs regulates the quality of the anti-viral antibody response.

Introduction

The features that separate protective adaptive immune responses from similar responses that fail to protect from infection have yet to be clearly delineated. Aside from important factors such as antigen structure or antibody specificity, it is widely believed that many aspects that define protective immunity are instructed by the innate immune system [1–4]. Presumably, pathogens and live vaccines trigger multiple pattern recognition receptors (PRRs) that induce the optimal set of signaling molecules for the regulation of protective adaptive immune responses. In contrast, adjuvant-based immunizations with subunit vaccines likely represent incomplete mimics of live vaccines that fail to replicate the necessary set of regulatory signals. As the nature and functions of these signals are incompletely understood, rational vaccine design is still facing considerable challenges. Consistent with this view, the highly successful live yellow fever vaccine YF-17D activates multiple PRRs that collectively define the cytokine profile and magnitude of both CD4 and CD8 T cell responses as well as antibody responses [5–7]. Likewise, recognition of RNAs uniquely associated with live bacteria can promote the magnitude and vaccine efficacy of T-dependent antibody responses [8–10]. Vaccination with live attenuated microbes is therefore still often considered the best way to elicit effective long-lasting cellular and humoral immunity [4,11–13].

A key feature that distinguishes viral infections from immunizations with subunit vaccines is the activation of cytosolic RNA or DNA-sensing PRRs during the course of viral infections. The Rig-I-like receptor (RLR) family of PRRs include the ubiquitously-expressed RNA-sensing helicases RIG-I and MDA5, which recognize microbial RNA in the cytosol [14]. Both receptors rely on the adaptor protein MAVS for the transmission of their signal and the induction of proinflammatory cytokines and interferon responses [14–16]. RLRs clearly play an essential function in the regulation of innate immunity to many RNA viruses as mice deficient of components of the RLR signaling pathway often suffer from uncontrolled viral replication and succumb to the infection. However, a clear understanding of RLR function in adaptive immunity has remained elusive as the uncontrolled viral replication complicates efforts to separate intrinsic functions of RLRs from the confounding variables of antigen load and pathology.

Infection of MAVS-deficient mice ($MAVS^{KO}$ mice) with West-Nile Virus (WNV), a single-stranded RNA virus of the flavivirus family, results in a dysregulated adaptive immune response [17–19]. In particular, $MAVS^{KO}$ mice generate poorly neutralizing antibodies against pathogenic WNV, even though they have higher WNV-specific antibody titers than wild-type controls, suggesting that MAVS may play a role in quality control of the antibody response to WNV [17]. This finding was surprising because WNV-mediated TLR activation should be sufficient for the generation of humoral immunity to WNV. However, interpreting this result as evidence for a direct link between MAVS-induced signals and the quality of neutralizing antibody responses is challenging because MAVS deficiency also leads to a significant increase in WNV viremia (>1000-fold) that causes severe pathology and death as well as an excess of viral antigens [17]. It remains therefore unclear whether MAVS directly contributes to humoral immunity to WNV.

To overcome the limitations of high viral titers associated with WNV infections of mice with deficiencies in innate signaling pathways, we infected $MAVS^{KO}$ mice with a single-round-of-infection mutant of pathogenic WNV called WNV-RepliVAX (RWN) [20]. This

mutant virus carries a deletion in the capsid gene and fails to generate infectious viral particles but produces all other viral proteins and RNA. Using this system, we show here that MAVS^{KO} mice fail to generate effective neutralizing antibody responses to RWN even under conditions of similar antigen loads. We show that this defect is caused by a T-dependent antibody response that is directed at the neutralizing epitope of WNV but displays a lower affinity for this epitope. Our data therefore suggest that MAVS-dependent signals directly influence the quality of the antiviral antibody response against WNV by calibrating the affinity of the neutralizing antibodies.

Results

Impaired neutralizing antibody response to RWN in RWN-infected MAVS^{KO} mice

To dissect the function of MAVS in the regulation of humoral immunity, we infected MAVS^{KO} mice and MAVS^{WT} controls with a replication-incompetent mutant of the pathogenic WNV-TX strain called WNV-RepliVAX (RWN) [21]. This mutant lacks a functional capsid gene and thus fails to produce infectious progeny but otherwise generates all viral proteins and RNA. RWN-infection of MAVS^{KO} mice in the footpads led to a WNV-E-specific IgM and IgG response at wild-type levels on day 8 post-infection (Fig 1A and 1B). The antibody response of MAVS^{KO} mice remained similar to MAVS^{WT} mice over the course of the primary antibody response (S1A–S1D Fig). MAVS^{KO} mice also efficiently produced WNV-E-specific IgG2b, IgG2c, and IgG3, the main IgG isotypes induced by WNV and RWN, although we noticed elevated but still relatively low titers of IgG3 on day 8 post infection (S1E and S1F Fig) [17,22]. Next, we determined whether sera from MAVS^{KO} mice on day 8 post infection were able to neutralize WNV prior to the infection of target cells *in vitro*. We chose this time point because WNV neutralization is thought to depend primarily on IgM during primary infections and IgM titers of RWN-infected animals peak at that time (S1A–S1D Fig) [23]. Surprisingly, we found that sera from RWN-infected MAVS^{KO} failed to neutralize the virus effectively when compared to MAVS^{WT} mice (Fig 1C). Importantly, the sera from MAVS^{KO} mice also showed a neutralization defect of WNV when the amounts of RWN-specific IgM and IgG titers were taken into account, as MAVS^{KO} mice exhibited a significantly lower neutralization index than MAVS^{WT} mice (neutralization divided by amount of virus-specific IgM + IgG) (Fig 1D). This finding was also true when the neutralization index was calculated based on the IgM or IgG titers alone (S2A and S2B Fig). Finally, we tested whether the antibody response of MAVS^{KO} mice is also defective between 14–28 days when WNV-E-specific IgG antibodies dominate. Indeed, sera from MAVS^{KO} mice failed to neutralize the virus effectively even at these later stages of the antibody response (S3 Fig).

Due to the repetitive nature of the envelope proteins on viral surfaces, many viruses can elicit a combination of T-dependent or T-independent antibody responses. Indeed, the primary antibody response to replicating WNV is initially independent of CD4^{+} T cells and becomes mainly T-dependent by day 10 [24]. As the kinetics of the antibody response to RWN may differ from that to WNV and MAVS is known to regulate components of the complement cascade, we wanted to ascertain that the observed impairment of virus neutralization by sera from RWN-infected MAVS^{KO} mice on day 8 is indeed due to a defect of the T-dependent antibody response itself. The neutralization defect of sera from RWN-infected MAVS^{KO} mice was complement-independent as virus neutralization by these sera was still inferior compared to sera from MAVS^{KO} mice following heat-inactivation of the sera (S4A Fig). Thus, we infected MHCII^{KO} and CD40^{KO} mice as well as wild-type controls with RWN and measured the ability of the sera from these mice to neutralize the virus. In contrast to sera from wild-type mice, sera

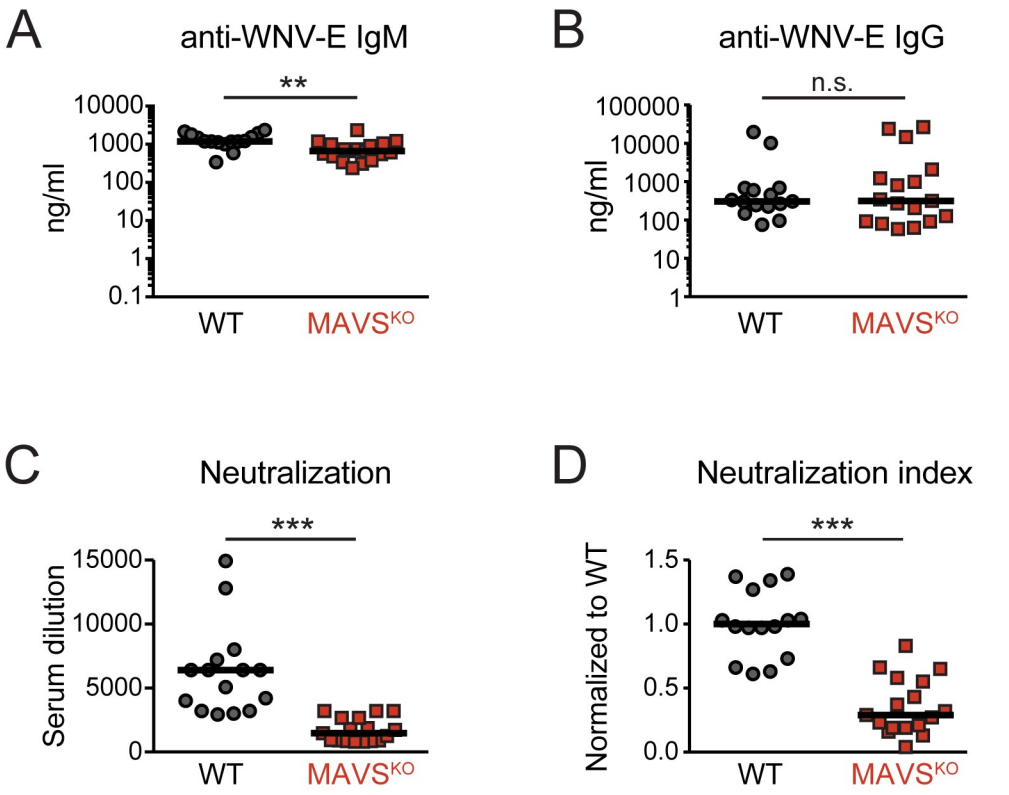

Fig 1. Impaired neutralizing antibody response in RWN-infected MAVS^{KO} mice. (A, B) WNV-E-specific IgM (A) and IgG (B) on day 8 after infection with RWN (10^5 pfu/footpad) as measured by ELISA. **(C)** Virus neutralization by sera of infected MAVS^{KO} and MAVS^{WT} mice. RWN was incubated with serial dilutions of sera prior to infection of Vero cells *in vitro*. The number of infected cells was determined 30–48 hours later by staining with an anti-WNV-E antibody. The reduction of infected cells by 90% was scored (PRNT90). **(D)** Neutralization index on day 8 post infection. The index normalizes virus neutralization to the total amount of WNV-E-specific antibodies in MAVS^{KO} and MAVS^{WT} mice. The index was calculated by dividing the dilution factor (PRNT90) of each mouse by the total amount of WNV-E-specific IgM and IgG of the same mouse. The data were normalized across multiple experiments to MAVS^{WT} mice. Each dot represents one mouse, the lines represent the median. **, $p < 0.005$; ***; $p < 0.0005$; n.s., not significant; Mann-Whitney test.

https://doi.org/10.1371/journal.ppat.1009009.g001

from either MHCII^{KO} or CD40^{KO} mice were completely devoid of any neutralizing activity to RWN (S4B and S4C Fig). Together, our data show that viral neutralization by sera from RWN-infected mice depends on the generation of T-dependent antibody responses and is unlikely to involve significant contributions of innate effector mechanisms such as the production of anti-microbial peptides or altered complement activation. Instead, MAVS regulates the quality of the anti-WNV antibody response.

RWN infection of MAVS^{KO} mice causes an increase in viral RNAs but not antigens

To test the nature of RWN infection in MAVS^{KO} mice compared to MAVS^{WT} mice, we infected mice with RWN and measured first the presence of viral RNA in the whole draining lymph nodes (dLNs, here: inguinal and popliteal LNs) by quantitative PCR using primer pairs that anneal in the viral WNV-E and NS4b genes. We found that dLNs from MAVS^{KO} mice contained significantly more viral RNA on day 1 post infection than those from MAVS^{WT} mice (Fig 2A). The amount of viral RNA rapidly declined afterwards and was barely detectable

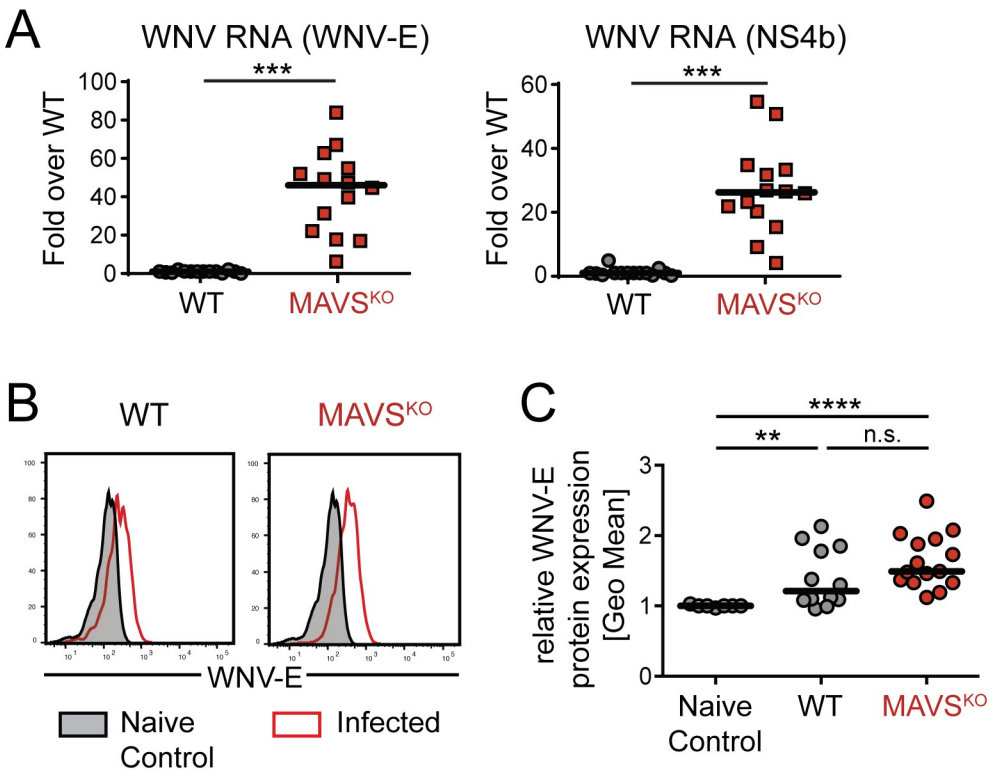

Fig 2. Similar levels of WNV-E protein in RWN-infected MAVS^{KO} and MAVS^{WT} mice. (A) Viral RNA levels in the dLNs on day 1 post infection with RWN (10^5 pfu/footpad) as measured by qPCR using primer pairs located in the WNV-E or NS4b genes of the viral genome. Data were normalized to the RNA level of RWN-infected MAVS^{WT} mice. **(B, C)** Production of WNV-E protein in cells from the dLNs of RWN-infected MAVS^{KO} and MAVS^{WT} mice. Cells from the dLNs were isolated 24 hours after infection and cultured for an additional 24 hours *in vitro*. The amount of WNV-E protein in the combined cell lysates and supernatants was quantified by flow cytometry using an anti-WNV-E bead assay. Samples from naïve mice or assay buffer were used as controls. **(B)** A representative experiment is shown. Shaded area represents the background staining of samples from uninfected animals, red lines represent RWN-infected animals. **(C)** Statistical summary of geometric means of multiple independent experiments. The data were normalized to the background staining of uninfected mice in each experiment. Each dot represents one mouse; the line is the median; n.s., not significant, ***, $p < 0.0005$, Mann-Whitney test.

https://doi.org/10.1371/journal.ppat.1009009.g002

by day 8 (S5 Fig). As RWN is restricted to a single round of infection, we conclude that MAVS^{KO} mice produce more viral RNA per infected cell without expanding the number of infected cells. RLR-mediated inhibition of protein translation during infection with RNA viruses is thought to occur independently of MAVS and instead may be regulated by the innate signaling adaptor STING [25]. We therefore determined whether the elevated levels of viral RNA in MAVS^{KO} mice also translate into more viral proteins in the dLNs. We isolated cells from the dLNs from MAVS^{KO} mice and MAVS^{WT} controls on day 1 post RWN-infection, cultured these cells for 24 hours *in vitro*, and measured the production of WNV-E during that time period in a flow cytometry-based bead assay. We used samples from naïve mice or assay buffer as negative controls. Cells from both MAVS^{KO} and MAVS^{WT} mice produced significant amounts of WNV-E compared to controls. However, we did not observe significant differences in WNV-E production between MAVS^{KO} and MAVS^{WT} mice, even though we noticed a modest trend towards higher WNV-E production in MAVS^{KO} mice (Fig 2B and 2C). Together, our data show that RWN infection of MAVS^{KO} mice leads to the expression of more viral RNA compared to MAVS^{WT} mice but does not significantly alter the levels of viral antigens. We conclude that RWN infection of MAVS^{KO} mice overcomes the caveats associated

with replication-competent WNV, namely severe pathology and abundance of viral antigens due to the uncontrolled viral replication in these mice.

Antibody-mediated virus neutralization of RWN-infected mice is independent of antigen loads

It is well-known that high antigen loads can affect the quality of the antibody responses [26,27]. In contrast to infections with replicating WNV, $MAVS^{KO}$ mice infected with RWN do not produce significantly higher amounts WNV-E protein in the dLNs than $MAVS^{WT}$ mice, suggesting that uneven antigen loads are not major drivers of the observed neutralization defect in RWN-infected $MAVS^{KO}$ mice. Nonetheless, as we noticed a trend towards higher levels of WNV-E expression in $MAVS^{KO}$ mice (Fig 2A and 2B and S5 Fig), we tested whether an increase of the infectious dose of RWN can impact the anti-WNV neutralization index in $MAVS^{WT}$ mice. We first compared $MAVS^{KO}$ mice infected with the standard dose of 10^5 Pfu per footpad to $MAVS^{WT}$ mice infected with a high dose of 10^6 Pfu per footpad to ensure that the chosen increased dose for $MAVS^{WT}$ mice leads to similar or higher levels of WNV-E protein in the dLNs. Cells from the dLNs of $MAVS^{WT}$ mice infected with the high dose did indeed express equivalent amounts of WNV-E protein as $MAVS^{KO}$ mice infected with the standard dose (Fig 3A). Importantly, an up to 10-fold increase of the infectious dose in $MAVS^{WT}$ mice did not impact neutralization efficiency of the antibody response as this did not negatively impact the neutralization index (Fig 3B). We thus conclude that the impact of MAVS on the quality of the antibody response in RWN-infected animals is independent of the antigen load.

Enhanced Tfh cell and GC B cell response to RWN in $MAVS^{KO}$ mice

In order to gain insights into the potential drivers for the impaired neutralizing antibody response, we next characterized the T and B cell response of RWN-infected $MAVS^{KO}$ mice on the cellular level. $MAVS^{KO}$ mice had normal absolute B cell numbers in the dLNs on day 8 after RWN infection (Fig 4A). However, germinal center (GC) B cells were more frequent in these mice (Fig 4B). Absolute $CD4^+$ T cell numbers were increased in the dLNs of $MAVS^{KO}$

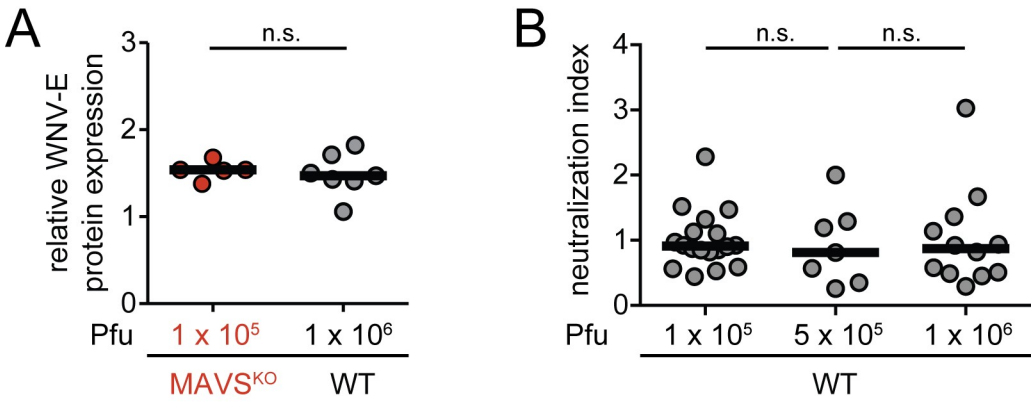

Fig 3. Increased antigen production does not impair virus neutralization. (A) Comparison of the viral load in the dLNs of $MAVS^{KO}$ mice infected with 10^5 Pfu RWN and $MAVS^{WT}$ mice infected with an increased dose of 10^6 Pfu RWN. Cells from the dLNs were isolated 24 hours after infection and cultured for an additional 24 hours *in vitro*. The amount of WNV-E protein in the combined cell lysates and supernatants was quantified by flow cytometry using an anti-WNV-E bead assay. **(B)** Increased doses of RWN do not impair virus neutralization in $MAVS^{WT}$ mice. Mice were infected with indicated doses of RWN. The amount of WNV-E-specific IgM and IgG as well as PRNT90 were determined in order to calculate the neutralization index. Shown are the combined data of 3 experiments. Each dot represents one mouse, the line represents the median. ns, not significant; Mann-Whitney test.

https://doi.org/10.1371/journal.ppat.1009009.g003

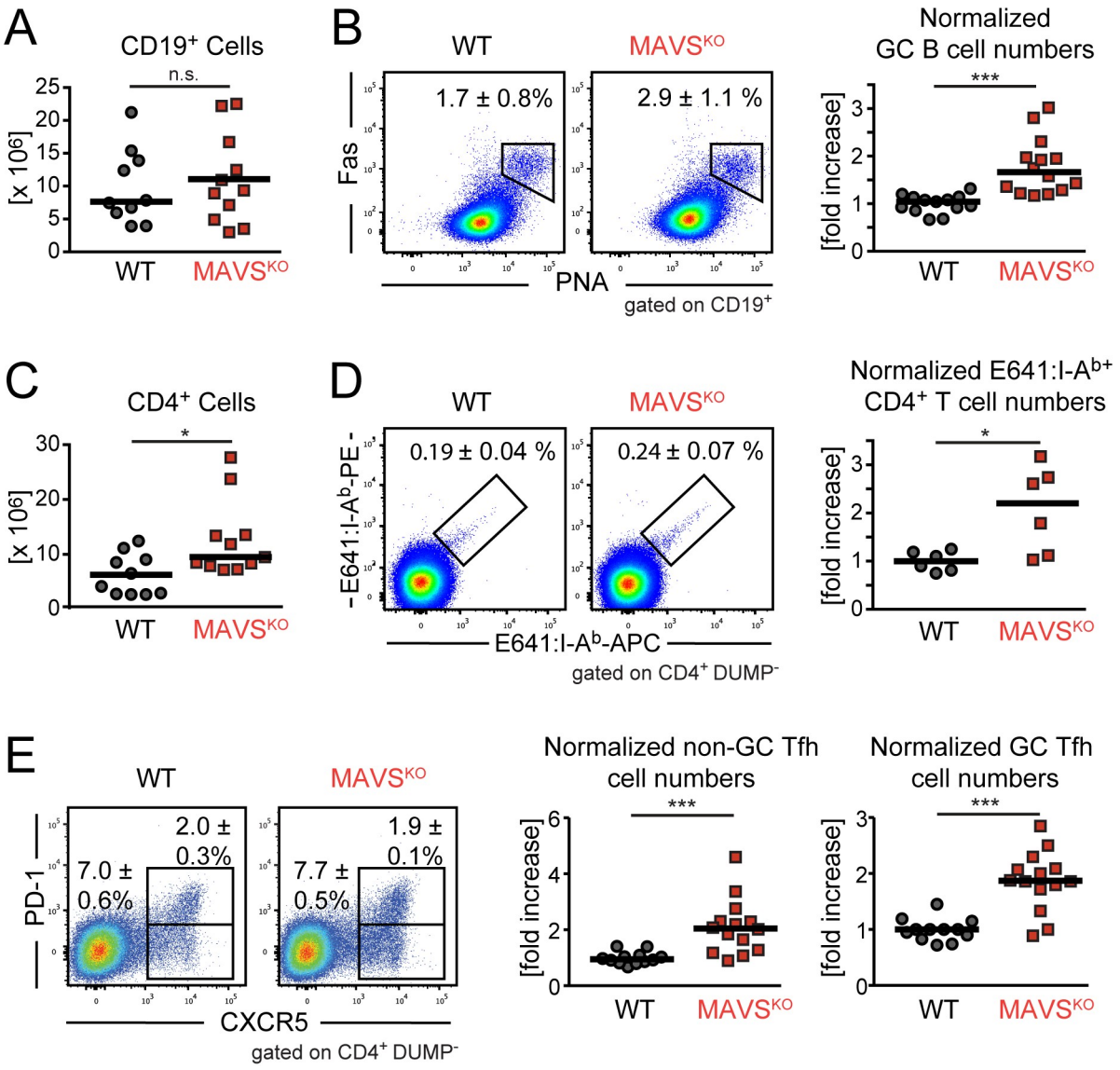

Fig 4. Enhanced GC B and CD4$^+$ T cell response to RWN in MAVS^{KO} mice. The cellularity of the dLNs from MAVS^{KO} and MAVS^{WT} mice was analyzed 8 days post RWN infection (10^5 pfu/footpad) by flow cytometry. **(A)** Total numbers of CD19$^+$ B cells. **(B)** Left panels: Frequency of Germinal Center (GC) B cells. Right panel: Total GC B cell numbers of 5 experiments normalized to the average of MAVS^{WT} mice in each experiment. **(C)** Absolute number of CD4$^+$ T cells. **(D)** Left panels: Frequency of E641:I-A^b class II tetramer$^+$ CD4$^+$ T cells specific for the immunodominant E641 epitope derived from WNV-E. Right panel: Total E641:I-A^{b+} CD4$^+$ T cells numbers of 3 experiments normalized to the average of MAVS^{WT} mice in each experiment. **(E)** Left panels: Frequency of non-GC CXCR5$^+$ PD-1$^-$ T follicular helper (Tfh) cells and CXCR5$^+$ PD-1$^+$ GC Tfh cells. Right panel: Total Tfh cell numbers of 5 experiments normalized to the average of MAVS^{WT} mice in each experiment. Frequencies are shown as mean ± SEM. Cell numbers: Each dot is one mouse, lines are the medians. *, $p < 0.05$; ***; $p < 0.0005$; n.s., not significant; Mann-Whitney test.

https://doi.org/10.1371/journal.ppat.1009009.g004

mice (Fig 4C). CD4$^+$ T cells specific for the immuno-dominant WNV epitope E641 were present in similar frequencies in MAVS^{KO} and MAVS^{WT} mice as shown by staining with E641:I-A^b MHC class II tetramers (Fig 4D). However, as the CD4$^+$ T cell compartment was enlarged in MAVS^{KO} mice, these mice contained significantly more E641:I-A^{b+} CD4$^+$ T cells in the dLNs than MAVS^{WT} controls (Fig 4D). Similarly, the frequency of both CXCR5$^+$ PD-1$^-$ non-GC Tfh cells and CXCR5$^+$ PD-1$^+$ GC Tfh cells did not change in MAVS^{KO} mice but the

numbers of both non-GC and GC Tfh cell were increased (Fig 4E). To test whether $CD4^+$ T cells responding to RWN are functional in $MAVS^{KO}$ mice, we isolated these cells from the dLNs on day 8 post infection and measured the expression of the Tfh cell-cytokine IL-21 directly or after restimulation with the E641 peptide in the presence of naïve splenocytes as antigen-presenting cells. These analyses revealed that $CD4^+$ T cells from $MAVS^{KO}$ mice expressed IL-21 at wild-type levels (S6A and S6B Fig). Restimulated $CD4^+$ T cells from $MAVS^{KO}$ mice and wild-type controls also produced IFN-γ at equal levels (S6C Fig). Together, our findings may imply that the qualitative defect of the antibody response to RWN in $MAVS^{KO}$ mice is caused by an impaired recruitment of WNV-E-specific B cells with high affinity into the response, either because of a defect that acts on B cells directly or a reduced selection pressure due to an increase in the numbers or function of non-GC or GC Tfh cells [28].

Altered cytokine production in the dLNs of $MAVS^{KO}$ mice

RLRs are major inducers of NF-κB-driven proinflammatory cytokines and type I and type III IFN responses. In fact, the induction of IFNs in particular often depends on the activation of RLRs in infections with RNA viruses. As such changes in the cytokine milieu may alter the generation of T or B cell responses in RWN-infected $MAVS^{KO}$ mice, we determined the expression of a selection of cytokines and IFNs in these mice. We measured the expression of cytokines, IFNs, and interferon-sensitive genes (ISGs) in the whole dLNs of $MAVS^{KO}$ and $MAVS^{WT}$ mice 24 hours after RWN-infection by qRT-PCR. We chose this time point because IFN responses peak early in viral infections and innate instruction of $CD4^+$ T cells and B cells is thought to occur at that time as well. Both naïve $MAVS^{KO}$ and $MAVS^{WT}$ mice expressed low but similar levels of the assayed genes (Fig 5 and S7A Fig). However, RWN-infected $MAVS^{KO}$ mice expressed more IL-1β, IL-6, and IFN-λ in the dLNs than infected $MAVS^{WT}$ controls, whereas infected $MAVS^{KO}$ and $MAVS^{WT}$ mice expressed equal amounts of type I IFNs and TNF-α (Fig 5A and 5B). Systemic type I IFNs in the serum of RWN-infected mice were only detectable by a type I IFN-sensitive bioassay and were not significantly different between $MAVS^{KO}$ mice and $MAVS^{WT}$ controls, suggesting that IFNs mainly act locally in RWN-infected mice (S8 Fig). Finally, ISG expression was unchanged in the dLNs of $MAVS^{KO}$ mice (Fig 5C). Proinflammatory cytokines remained expressed at the same levels in $MAVS^{KO}$ and $MAVS^{WT}$ mice 48 hours post infection, while IFNs and ISGs were, as expected, downregulated (S7B–S7D Fig). Together, the data suggest that inflammatory mediators are not uniformly dysregulated in $MAVS^{KO}$ mice and that the expression of specific cytokines known for their ability to promote Tfh or B cell immunity such as IL-1β and IL-6 is increased in these mice [29,30]. Of note, we did not observe that specific cytokines, IFNs, or ISGs were downregulated in $MAVS^{KO}$ mice, suggesting that the expression of these genes is driven by other PRRs than RLRs.

Antibodies specific for the neutralizing epitope in the WNV-E protein are efficiently generated in $MAVS^{KO}$ mice

Alterations in the Tfh and B cell response of $MAVS^{KO}$ mice (Fig 4) suggested that the entry or selection of WNV-E-specific B cells into the response is affected in these mice. Although RWN-infected $MAVS^{KO}$ mice produce similar amounts of WNV-E-specific antibodies, they may preferentially generate antibodies that are directed at non-neutralizing epitopes. The major neutralizing epitope of WNV is located in the lateral ridge (LR) epitope of the domain III (DIII) of WNV-E [31–33]. Thus, we used recombinant DIII protein as antigen in ELISAs to test whether the serum of $MAVS^{KO}$ and $MAVS^{WT}$ mice contain similar amounts of

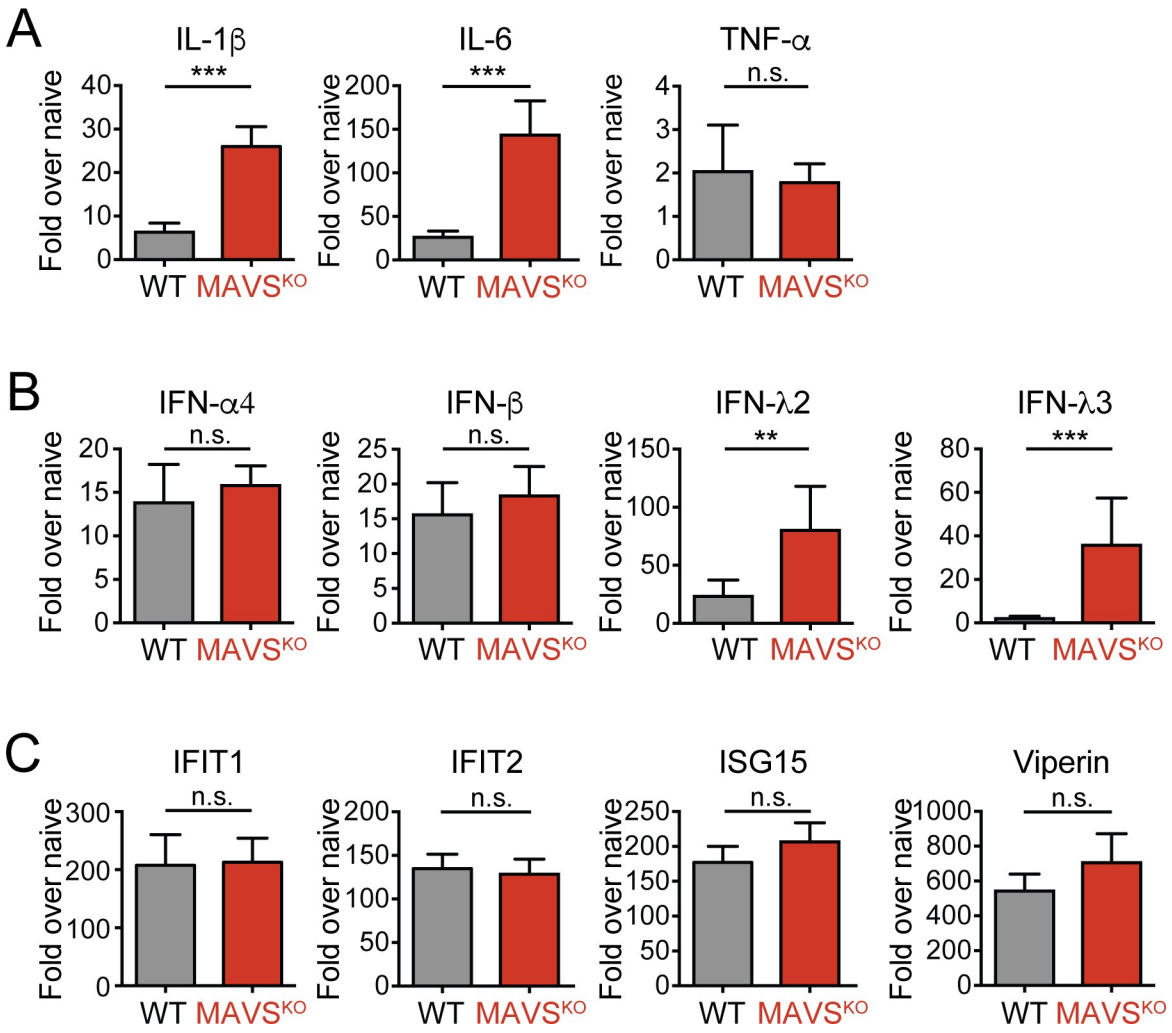

Fig 5. Production of cytokines and interferon-stimulated genes (ISGs) in the dLNs of MAVS^{KO} mice. **(A)** Expression of IL-1β, IL-6, and TNF-α mRNA RWN-infected MAVS^{KO} and MAVS^{WT} mice. **(B)** Expression of type I and type III IFNs mRNA in RWN-infected MAVS^{KO} and MAVS^{WT} mice. **(C)** Expression of representative ISGs in RWN-infected MAVS^{KO} and MAVS^{WT} mice. **(A-C)** mRNA was isolated from whole dLNs cells of mice 24 hours after infection with 10^5 Pfu RWN per footpad and measured by qPCR. Shown is the expression over that of dLNs from naïve WT mice. Expression of GAPDH was used to normalize the samples. Shown are the combined data of at least 4 experiments using 8–20 mice/genotype **, $p < 0.005$; ***, $p < 0.0005$; Mann-Whitney test.

https://doi.org/10.1371/journal.ppat.1009009.g005

DIII-LR-specific antibodies. We also measured the antibody titers specific for a mutant form of DIII with an altered LR epitope (DIII-K307E/T330I) that abrogates the binding of DIII-LR-specific antibodies. We found that the levels of both DIII-specific IgM and IgG remained unchanged in MAVS^{KO} mice (Fig 6A). The same was true for anti-DIII-K307E/T330I antibodies in these mice (Fig 6B). Consistent with previous findings, the anti-DIII-K307E/T330I antibody titers were much lower than those specific for wild-type DIII, suggesting that the majority of anti-DIII antibodies in both MAVS^{KO} and MAVS^{WT} mice are directed against the neutralizing DIII-LR epitope [34]. Importantly, the ratio of antibodies bound to DIII versus DIII-K307E/T330I was also similar in MAVS^{KO} and MAVS^{WT} mice (Fig 6A and 6B). A recalculation of the neutralization index (Fig 1D) with the anti-DIII antibody titers reinforced the notion that the neutralizing Ab response is compromised in MAVS^{KO} mice (S9 Fig). Together, these findings demonstrate that MAVS^{KO} mice produce antibodies against WNV with similar

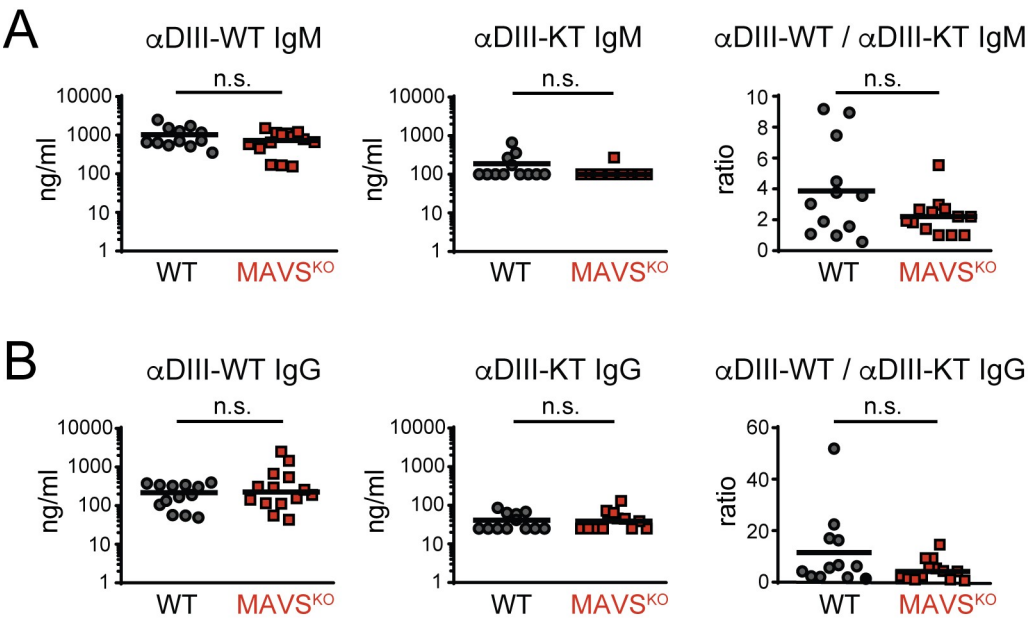

Fig 6. Normal specificity of the antibody response of MAVS^{KO} mice to the neutralizing lateral ridge (LR) epitope in the WNV-E DIII domain. (A, B) The antibody response of RWN-infected MAVS^{KO} and MAVS^{WT} mice was measured 8 days post infection. Shown are the titers of IgM **(A)** and IgG **(B)** specific for the WT DIII domain or the mutant form DIII-KT containing loss-of-function mutations in the neutralizing LR epitope (DIII-K307E/T330I). Ratios represent the excess of antibodies directed at the neutralizing epitope over the amount of non-neutralizing antibodies directed at the DIII domain. Combined data of 4 experiments. Each data point is one mouse, the line is the median; n.s., not significant; Mann-Whitney test.

https://doi.org/10.1371/journal.ppat.1009009.g006

specificities as MAVS^{WT} mice and a lack of antibodies against the neutralizing DIII-LR epitope is not responsible for the neutralization defect of MAVS^{KO} mice.

Decreased avidity of anti-DIII antibodies in MAVS^{KO} mice

Given the unchanged specificity of the antibody response in MAVS^{KO} mice, we hypothesized that the defect in virus neutralization of MAVS^{KO} is caused by a lower avidity of the neutralizing antibodies in these mice. To test this, we measured the avidity of the antibodies against the DIII domain by ELISA in the presence of increasing amounts of NaSCN to enhance the stringency of antibody binding. For IgM, we also reduced the binding avidity by diluting the recombinant DIII antigen with BSA. Consistent with previous results (Fig 1A), we did not find any differences in the total anti-DIII IgM titers between MAVS^{KO} and MAVS^{WT} mice (Fig 7A). However, upon dilution of DIII with BSA and increasing concentration of NaSCN, we observed a successive reduction of the anti-DIII IgM titers from sera of RWN-infected MAVS^{KO} mice while sera from MAVS^{WT} mice retained their ability to bind to DIII significantly better (Fig 7A). The quantification of these results, in which we expressed the amount of high avidity anti-DIII IgM as percentage of total anti-DIII in each mouse, confirmed this result (Fig 7B). In contrast to the anti-IgM response of MAVS^{KO} mice, we did not observe major differences in the anti-DIII IgG response of these mice compared to MAVS^{WT} controls (Fig 7C and 7D). The latter observation was consistent with the notion that the primary antibody response to WNV is dominated by IgM whereas somatically mutated high-affinity IgG responses emerge late in the primary response and are mainly required for protection from secondary challenges [23,35,36]. Together, these results show that MAVS-deficiency results in a qualitatively inferior primary antibody response due to a reduced avidity to the neutralizing

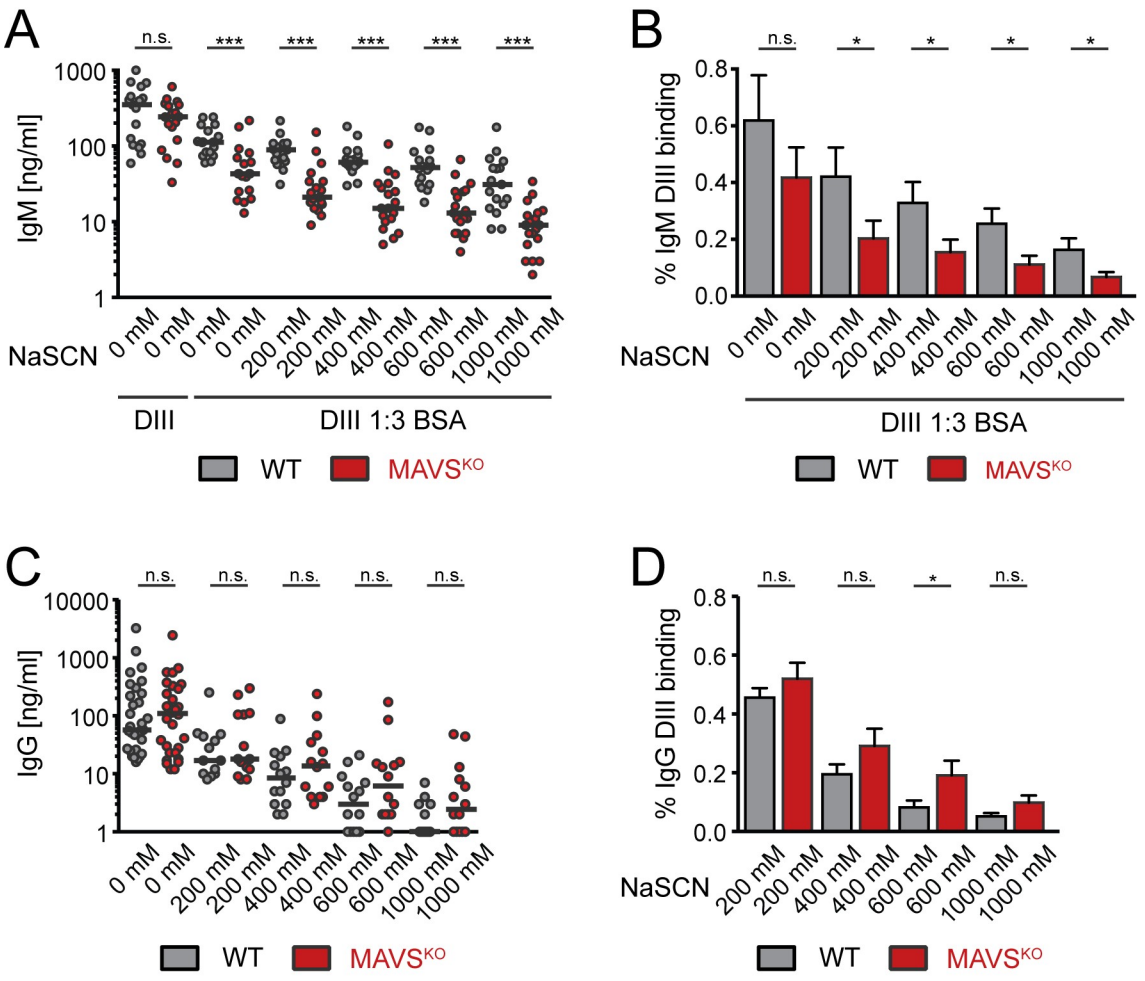

Fig 7. Impaired avidity of the IgM response to the DIII domain of WNV-E protein in RWN-infected MAVS^{KO} mice. (A, B) DIII-specific IgM titers from RWN-infected mice were measured by ELISA in the presence of BSA to reduce binding avidity and increasing amounts of NaSCN to enhance stringency of binding. Recombinant DIII protein was used as antigen. Shown are the absolute titers (A) and the titers as fraction of the total amount of DIII-specific antibodies in the absence of BSA and NaSCN for each mouse (B). **(C, D)** Same as before for DIII-specific IgG. Shown are the combined data of 4 experiments. Each dot represents one mouse, the line is the median. *, $p < 0.05$; ***, $p < 0.0005$; n.s., not significant; Mann-Whitney test.

https://doi.org/10.1371/journal.ppat.1009009.g007

LR epitope of WNV-E protein. By extension, this suggests that the reduced avidity is a reflection of a lower affinity of the antibodies participating in the response as the binding properties of each isotype class are determined by the affinity of the antibody variable region. In light of the defective IgM response, which consists mostly of unmutated antibodies, these findings also imply that MAVS directly affects the recruitment of B cells into the immune response.

Discussion

In contrast to the better-known functions of transmembrane PRRs, the mechanisms by which cytosolic PRRs regulate adaptive immunity are still poorly understood. Previous work suggested that the detection of viral RNA by RLRs and their signaling adaptor MAVS is an important step in the control of adaptive immunity to pathogenic WNV [17,18,37]. While these results seemingly established a link between MAVS signaling and the generation of protective adaptive immune response, it was difficult to attribute a specific role to MAVS in the

regulation of such responses as the unrestricted viral replication in the absence of MAVS-dependent innate immune defenses results in strongly elevated levels of viral antigens and RNAs as well as severe pathology and death [17]. To overcome these complications, we have used a replication-incompetent mutant of a pathogenic WNV called RepliVAX-WN (RWN) to study the functions of MAVS in anti-viral humoral immunity.

We show here that MAVS-deficiency results in a defective neutralizing antibody response to RWN. This defect becomes already apparent early in the response, when IgM dominates, but continues to affect the later stage of the response as well. Although the RLR/MAVS signaling pathway is known to regulate the release of serum components such as specific members of the complement cascade, we show that the MAVS-dependent effects on WNV neutralization impact T-dependent antibodies, consistent with the previously observed important contribution of T-dependent antibodies to the overall humoral immune response to WNV [24,38]. MAVS-deficiency does not alter the overall magnitude of the antibody response, in contrast to RWN-infected mice deficient of MyD88, the signaling adaptor of most TLRs and members of the IL-1 receptor family [39]. Instead, the lack of MAVS reduces the overall avidity and ultimately the affinity of the IgM response, the main isotype responsible for protection during primary infection, to the neutralizing LR epitope of the DIII domain despite otherwise normal anti-DIII antibody titers [31,33,40–44]. This feature is the likely cause for the impaired WNV neutralization in $MAVS^{KO}$ mice, as antibody affinity defines the antibody occupancy rate of the WNV virion and thus is a major factor that determines WNV neutralization [45].

In principle, a low antibody occupancy of the WNV virions due to a reduced affinity of the antibodies against WNV in $MAVS^{KO}$ mice may cause an antibody-mediated enhancement (ADE) of infection upon Fc receptor-mediated endocytosis [40,45–48]. ADE has been observed in the context of several flavivirus infections, most notably in Dengue virus infection, where it has been suggested to contribute to hemorrhagic fever during secondary infection [49–54]. We did not test ADE in our *in vitro* system of virus neutralization as Vero cells lack Fc receptors. Although ADE remains a potential possibility in our experimental system, ADE may not play as prominent a role in WNV pathogenesis unlike other flavivirus infections, particularly since the effects of ADE during WNV infection *in vivo* may be limited by the complement component C1q [40,55–57].

High antigen loads and the associated abundant formation of immune complexes have been recognized since the early days of B cell immunology for their potential to impair the overall affinity of the antibody response [26,27]. While such a scenario may contribute to the impaired antibody response in the context of uncontrolled replication of pathogenic WNV, it is an unlikely factor in infections of $MAVS^{KO}$ mice with RWN. Here, the replication-incompetent nature of this WNV mutant results in a similar cellular tropism in mice as wild-type controls, which differs from WNV-infected mice with deficiency in type I IFN responses [58]. Despite elevated levels of viral transcripts in the dLNs, we observed only a modest increase of WNV-E protein production in $MAVS^{KO}$ mice early in the infection. These findings are consistent with a recent study indicating that the RIG-I/MDA5-mediated suppression of protein translation following infection with RNA viruses depends on the signaling adaptor STING instead of MAVS [25]. The mere increase in the infectious dose did not alter the quality of the neutralizing antibody response. Thus, the defect of the neutralizing antibody response in RWN-infected $MAVS^{KO}$ mice is not a consequence of a fundamental change in the antigen load or pathology and instead is likely caused by an altered immune regulation by cytokines or other signaling molecules in the absence of MAVS. Consistent with this view, a recent study of $MAVS^{KO}$ mice infected with a replicating non-pathogenic strain of WNV did not impair the quality of the antibody response, even though these mice exhibited increased viral titers [59].

At the present time, it remains unclear how MAVS regulates the quality of the antibody response. Although we did not resolve the cytokine profile of the individual cell populations in the dLNs, our data nonetheless indicate that several cytokines are upregulated in RWN-infected $MAVS^{KO}$ mice, presumably through the activity of other PRRs such as TLRs. One possibility may be that the altered cytokine environment in the dLNs of RWN-infected $MAVS^{KO}$ mice directly influences the ability of B cells to become activated. Indeed, both type I and type III IFNs can promote B cell responses directly by facilitating B cell receptor activation or indirectly by regulating the B cell-intrinsic activity of TLR7 and other PRRs [60–62]. Such signals may facilitate the activation of low affinity B cells that usually would be prevented from participating in the response. In this context, it is interesting that MAVS affects the quality of the neutralizing antibody response to the pathogenic WNV-TX strain and its derivative RWN, whereas it does not seem to play the same function in infections with the non-pathogenic WNV-MAD or the attenuated NS4b-P38G strains of WNV [17,19,59]. However, it is important to highlight that these latter strains do not modulate type I IFN responses, unlike pathogenic strains [19,59,63–65]. The divergent interference with the IFN signaling pathway of these strains thus further points towards a function of IFNs in the regulation of the anti-WNV antibody response.

An additional possibility is that altered cytokine profiles may lead to the promotion of an enhanced Tfh cell response. Indeed, we observed increased numbers of antigen-specific $CD4^+$ T cells as well as Tfh cells in RWN-infected $MAVS^{KO}$ mice. Here, the observed upregulation of IL-1 and IL-6 may help $CD4^+$ T cells to overcome Treg-mediated suppression and promote their differentiation into more effective Tfh cells [30,66,67]. The consequence of this scenario may therefore be a reduced competition of cognate B cells for Tfh cell help that leads to the entry of low affinity B cells into the immune response. Such a checkpoint is usually recognized in the context of a GC response. Here, the selection of high affinity B cells depends on their more successful access to limited Tfh cell help and becomes less stringent when T cell help is abundant [28,68]. However, a similar checkpoint is thought to occur already at the T-B border before cognate B cells re-enter the B cell follicle [69]. The reduced affinity of neutralizing IgM in $MAVS^{KO}$ mice therefore points towards a GC-independent event and may suggest that MAVS already prevents the recruitment of low affinity B cells into the anti-WNV immune response at this early stage by limiting the number of non-GC Tfh cells, thus facilitating the production of an antibody response with overall higher affinity to the neutralizing DIII-LR epitope.

IgM is the major isotype responsible for humoral immunity during primary WNV infection, whereas class-switched and somatically mutated IgG antibodies are thought to be more relevant for secondary WNV infection [23]. RLR ligands can promote increased immunogenicity and affinity maturation of IgG responses in protein immunizations [70]. Although the present work centered on the antibody response relevant for the control of primary infection, we also analyzed the impact of MAVS on the IgG response to WNV, particularly since we noted enlarged GC Tfh cell and GC B cell compartments in $MAVS^{KO}$ mice early in the response. At that stage, we did not observe a reduction of the affinity of DIII-LR-specific IgG antibodies in these mice in contrast to IgM. Such a lack of phenotype in the early IgG response may not be surprising because IgG titers are low and affinity maturation has just started. Nonetheless, we show that $MAVS^{KO}$ mice also have a defect in the mature neutralizing antibody response to WNV when IgG antibodies dominates, suggesting that MAVS not only regulates the recruitment of WNV-E-specific B cells into the response but also affinity maturation in the GC itself. Our findings thus provide a mandate to explore the regulation of GC responses by MAVS in more detail in future studies.

Regardless of the specific circumstances that promote the production of low affinity antibodies in RWN-infected $MAVS^{KO}$ mice, it is likely that this effect is caused by an absence of

MAVS in myeloid cells. This argument rests on the finding that myeloid cells are much more frequently infected by WNV than lymphocytes [58,59]. This view is also attractive because myeloid cells and DCs in particular orchestrate the early events of $CD4^+$ T cell responses [71]. Recent results with extracellular bacterial infections demonstrate that phagocytosed microbial RNA can be sensed by a combination of transmembrane PRRs such as TLR3 and cytosolic PRRs such as NLRP3 that cooperate to induce IL-1 and type I IFN for the regulation of Tfh responses [8–10]. Such regulatory circuits have been shown to affect primarily the magnitude of the antibody response, whereas our study demonstrates a role for the sensing of microbial RNA in the quality of the antibody response. Nonetheless, these findings may therefore set a precedent for the general recognition of microbial RNAs by phagocytes and provide a conceptual basis for the understanding of RLR signaling pathway in the regulation of antibody responses. Future experiments will address the questions about the origin and nature of the MAVS-dependent signals required for the regulation of the antibody response to WNV.

Material and methods

Ethics statement

Mouse studies were carried out in strict accordance with the recommendations in the Guide for the Care and Use of Laboratory Animals of the National Institutes of Health. The University of Arizona is an AAALAC international accredited animal care organization and all experiments were approved by the Institutional Animal Care and Use Committee of the University of Arizona under protocol 14–521.

Mice

$MAVS^{KO}$ mice, $MHCII^{KO}$ mice, and $CD40^{KO}$ mice were kept on a C57BL/6 background under SPF conditions [72–74]. Experimental mice and wild-type controls were cohoused immediately following weaning. The mice were analyzed between 7–12 weeks of age and involved both sexes.

Virus production and mouse infections or immunizations

The single-round-of-infection mutant of WNV (WNN-RepliVAX, RWN) has been described before [21]. This WNV-TX-derived virus carries an inactivated capsid gene and requires passaging over capsid-expressing BHK cells for the production of infectious virions. BHK cells were infected with 0.05 MOI of RWN and the supernatants were harvested 48–96 hours later. RWN titers were determined by infecting fresh Vero cells with serial dilutions of RWN and subsequent intracellular staining for infected cells with a biotinylated humanized anti-WNV-E antibody (hE16-biotin) followed by Streptavidin-horseradish peroxidase (HRP) [32] or, alternatively, with purified hE16, followed by anti-human IgG2a antibody. HRP-positive cells were detected with the TrueBlue substrate. Unless otherwise noted, mice were infected with RWN subcutaneously in the footpads with a dose of 1×10^5 Pfu per footpad. When indicated, mice were infected with 5×10^5 Pfu RWN and 1×10^6 Pfu RWN or immunized with 50 μg Ovalbumin and 5 μg LPS in Incomplete Freund's Adjuvant (all Sigma Aldrich, St. Louis, MO).

Virus neutralization

The assay to measure the ability of serum to neutralize WNV has been described before [75]. Briefly, 2000 pfu/ml RWN were incubated with serial dilutions of serum from RWN-infected mice for 2 hours at room temperature and subsequently used to infect Vero cells. The number of infected cells was assessed 30–48 hours later by staining for the expression of WNV-E

protein using an anti-WNV-E antibody (E16-biotin). Scored was the lowest dilution factor of serum necessary to achieve a reduction of 90% of infected cells compared to cells infected with WNV without prior serum incubation (PRNT90).

Antibodies and other reagents

Antibodies against CD3ε, CD4, CD8, CD11b, CD11c, CD25, CXCR5, PD-1, CD19, B220, and FoxP3 were purchased from BD Biosciences (San Diego, CA), ThermoFisher (Waltham, MA), or Biolegend (San Diego, CA). PNA was obtained from Vector Laboratories (Burlingame, CA). E641:I-A^b tetramers and recombinant DIII and DIII-K307E/T330I were kindly provided by M. Kuhns (University of Arizona) and D. Bhattacharya (University of Arizona), respectively [34,76].

Surface and intracellular staining

Cells were stained with indicated antibodies for 15 min on ice for cell surface staining. For CXCR5 and E641:I-A^b tetramer staining, cells were incubated for 45 min at room temperature. Stainings for intracellular antigens were performed with the BD Bioscience or Thermofisher (for FoxP3) intracellular staining kits. Cells were analyzed on a LSRFortessa flow cytometer (BD Bioscience, San Diego, CA) and the FlowJo software (Tree Star).

Detection of WNV-E protein

For the detection of WNV-E antigen levels in RWN-infected mice, 1–2 x 10^7 cells from the dLNs were isolated 24 hours after infection and cultured for an additional 24 hours *in vitro*. Subsequently, supernatants and cells were subjected to one freeze-thaw cycle at -80˚C to release RWN virions from the infected cells. After a centrifugation step, the supernatants were incubated with anti-mouse IgG2a-coupled LEGENDplex beads (Biolegend) that had been coated with the anti-DII/III E60 antibody at a concentration of 1 μg/100 μl of beads. Binding of WNV-E protein to the beads was detected by flow cytometry with the biotinylated anti-DIII hE16 antibody, followed by SA-PE. Samples from naïve mice or standards with and without recombinant WNV-E protein were used as controls.

T Cell Isolation, restimulation, and cytokine expression

The functional analysis of $CD4^+$ T cell responses has been published previously [66]. Briefly, $CD4^+$ T cells were MACS-purified from the draining lymph nodes with anti-CD4 (Miltenyi Biotec, Auburn, CA). Subsequently, isolated $CD4^+$ T cells were used to directly measure cytokine gene expression by qPCR. Alternatively, 2 x 10^5 $CD4^+$ T cells/well were cultured in 96-well U-bottom plates in the presence of 5μg E651 peptide and 3 x 10^5 naïve splenocytes as antigen-presenting cells. IL-21 production in the cultures was measured three days later by either qPCR. IFN-γ protein was measured by ELISA with an anti-mouse IFN-γ capture antibody, followed by an biotinylated anti-mouse IFN-γ detection antibody, and subsequently streptavidin-conjugated horseradish peroxidase (SA-HRP) and TMB substrate (both BD Bioscience, San Diego, CA).

Quantitative PCR

RNA was isolated from the dLNs following infection with RWN and converted into cDNA. Quantitative PCR was performed using the PerfeCTa SYBR Green Fastmix (Quantabio, Beverly, MA) on a StepOne Real-time PCR system (Applied biosystems, Foster City, CA). PCR

products were amplified with the following primer pairs: Cytokines: IL-1β-F 5'-TGAGCACCT TCTTTTCCTTCA and IL-1β-R 5'-TGTTCATCTCGGAGCCTGTA; IL-6-F 5'-GTTCTCTGG GAAATCGTGGA and IL-6-R 5'-TTTCTGCAAGTGCATCATCG; TNF-α-F 5'-CCCCAAAG GGATGAGAAGTT and TNF-α-R 5'-TGGGCTACAGGCTTGTCACT; IFN-α4-F 5'-AGGAC AGGAAGGATTTTGGA and IFN-α4-R 5'-GCTGCTGATGGAGGTCATT; IFN-β-F 5'-CAC AGCCCTCTCCATCAACT and IFN-β-R 5'- GCATCTTCTCCGTCATCTCC; IFN-λ2-F 5'-CAGAGCCCAGGTCCCCGA and IFN-λ2-R 5'-CACACTTGAGGTCCCGGGT; IFN-λ3-F 5'-CAGAGCCCAAGCCCCCGA and IFN-λ3-R 5'-CTTGAGGTCCCGGAGGAG; IFIT1-F 5'-GCTGAGATGTCACTTCACATGG and IFIT1-R 5'-CACAGTCCATCTCAGCACACT; IFIT2-F 5'-AGTACAACGAGTAAGGAGTCACT and IFIT2-R 5'-AGGCCAGTATGTTGCA-CATGG; ISG15-F 5'-GGTGTCCGTGACTAACTCCAT and ISG15-R 5'-TGGAAAGGG-TAAGACCGTCCT; and RSAD2-F 5'-TGCTGGCTGAGAATAGCATTAGG and RSAD2-R 5'-GCTGAGTGCTGTTCCCATCT; WNV proteins: E-F 5'-GGCTTCCTTGAACGACCTAA and WNV-E-R 5'-CGTGGCCACTGAAACAAAAG; and NS4b-F 5'-AACCCGTCTGTGAAG ACAGT and NS4b 5'-ATAGACATGACAACCAACCC. Primers for IL-21 have been published previously [30].

IFN Bioassay

IFN activity was measured by a standard assay quantifying the protection of cells from cytopathic effects (CPE) of vesicular stomatitis virus (VSV). L929 cells were plated on 96-well tissue culture plates and incubated for 24 hours at 37 ˚C. IFN-α2 standard was titrated and serum samples were serially diluted before incubation with VSV on confluent L929 cells for 24 hours. The cells were fixed with paraformaldehyde and stained with a solution containing crystal violet dye. The protection of cells from CPE by each serum sample was scored and compared to IFN-α2 standard samples to establish a concentration value for type I IFN in the serum in Units/ml.

Immunoglobulin ELISA

Detection of WNV-specific antibodies was based on ELISAs with recombinant WNV-E, DIII, or DIII-KT as antigens. Production of these reagents followed published protocols [77,78]. Briefly, DIII proteins were expressed in BL21(DE3) *E. coli* cells, refolded from inclusion bodies by oxidative refolding, and purified by size exclusion. AviTag-DIII protein was biotinylated and purified again by size exclusion. Serial dilutions of serum from RWN-infected mice were applied to plates coated with recombinant WNV-E, DIII; or DIII-KT proteins. Bound RWN-specific antibodies were detected with biotinylated goat anti-mouse IgM, IgG, IgG2b, IgG2c, or IgG3 (Southern Biotech, Birmingham, AL), followed by streptavidin-conjugated horseradish peroxidase (SA-HRP) and TMB substrate (both BD Bioscience, San Diego, CA). Anti-mouse Ig(H+L) (Southern Biotech, Birmingham, AL) and serial dilutions of mouse IgM and IgG2c (Southern Biotech, Birmingham, AL) were used for standards. High-affinity antibodies were measured similarly using plates coated with recombinant DIII alone or diluted 1:3 with BSA. After the initial binding, low affinity antibodies were washed off by incubating the samples for 15 min in presence of increasing amounts of NaSCN before detection with biotinylated goat anti-mouse IgM or IgG, followed by SA-HRP.

Statistical analysis

All experiments were performed independently three or more times. Statistical significance was determined with a Mann-Whitney test or Kruskal-Wallis test using the Prism6 software

(GraphPad). Number of asterisks represents the extent of significance with respect to the p value.

Supporting information

S1 Fig. Time course of WNV-E-specific antibody titers in RWN-infected mice. (A, B) WNV-E-specific IgM (A) and IgG (B) response on day 3 after infection with RWN (10^5 pfu/footpad) as measured by ELISA. Wild-type sera from day 8 were used as positive control. **(C, D)** WNV-E-specific IgM (C) and IgG (D) response over the course of 28 days after infection with RWN (10^5 pfu/footpad) as measured by ELISA. **(E, F)** WNV-E-specific IgG2b, IgG2c, and IgG3 titers on day 8 (E) and day 14 (F) post infection. Each dot represents one mouse, the lines represent the median. Shown are the combined data of 2–5 independent experiments. *, $p < 0.05$; **; $p < 0.005$; ***; $p < 0.0005$; n.s., not significant; Mann-Whitney test.
(TIF)

S2 Fig. Defective virus neutralization by sera from RWN-infected $MAVS^{KO}$ mice. (A, B) Neutralization index calculated based on serum-specific levels of WNV-ENV-specific IgM **(A)** or IgG **(B)** titers on day 8 after infection. The data were normalized across multiple experiments to WT mice. Each dot represents one mouse, the lines represent the median. **, $p < 0.005$; ****; $p < 0.00005$; n.s., not significant; Mann-Whitney test.
(TIF)

S3 Fig. Impaired neutralizing antibody response in RWN-infected $MAVS^{KO}$ mice 14–28 days after infection. (A) Virus neutralization by sera of infected $MAVS^{KO}$ and $MAVS^{WT}$ mice. RWN was incubated with serial dilutions of sera prior to infection of Vero cells *in vitro*. The number of infected cells was determined two days later by staining with an anti-WNV-E antibody. The reduction of infected cells by 90% was scored (PRNT90). **(B)** Neutralization index reflecting virus neutralization relative to the total amount of WNV-E-specific antibodies in $MAVS^{KO}$ and $MAVS^{WT}$ mice. The index was calculated by dividing the dilution factor (PRNT90) of each mouse by the total amount of WNV-E-specific IgM and IgG of the same mouse. The data were normalized to the average of sera from $MAVS^{WT}$ mice on day 14. Each dot represents one mouse, the lines represent the median. Shown are the combined data of two independent experiments. *, $p < 0.05$; **, $p < 0.005$; ***; $p < 0.0005$; Mann-Whitney test.
(TIF)

S4 Fig. Serum neutralization of RWN is mediated by a T-dependent antibody response. (A) Virus neutralization before and after heat-inactivation (HI) to exclude complement-mediated effects. Shown are the dilution factors that resulted in a 90% reduction of infection of target cells with RWN *in vitro* (PRNT90) and the neutralization index that accounts for the anti-WNV-E IgM and IgG titers in each mouse. **(B)** $MHCII^{KO}$ and **(C)** $CD40^{KO}$ mice as well as WT controls were infected with 10^5 Pfu of RWN in the footpads. Serum was collected 8 days later to measure the dilution factor. Shown are the combined data of two independent experiments. Each dot is one mouse. *, $p < 0.05$; **, $p < 0.005$; ***, $p < 0.0005$; ****, $p < 0.00005$; Mann-Whitney test.
(TIF)

S5 Fig. RWN-infected cells in the dLNs disappear quickly after infection. Viral RNA levels in the dLNs over the course of 8 days post infection with RWN (10^5 pfu/footpad) as measured by qPCR using primer pairs located in the WNV-E gene of the viral genome. Data were normalized to the RNA level of RWN-infected $MAVS^{WT}$ mice on day 1 post infection.
(TIF)

S6 Fig. Normal $CD4^+$ T cell response in RWN-infected $MAVS^{KO}$ mice. **(A)** Expression of IL-21 in $CD4^+$ T cells isolated on day 8 from the dLNs of $MAVS^{KO}$ mice and $MAVS^{WT}$ controls as measured by qPCR. Shown is the expression over that of naïve $MAVS^{WT}$ mice. Expression of GAPDH was used to normalize the samples. **(B)** Expression of IL-21 in isolated $CD4^+$ T cells from the dLNs three days after restimulation with E641 in the presence of naïve splenocytes as antigen-presenting cells as measured by qPCR. **(C)** Production of IFN-γ by isolated $CD4^+$ T cells from the dLNs following the restimulation with E641 as measured by ELISA. Shown are the combined data of three independent experiments representing a total 6–10 mice per genotype. n. s., not significant; Mann-Whitney test.
(TIF)

S7 Fig. Production of cytokines and interferon-stimulated genes (ISGs) in the dLNs of naïve $MAVS^{KO}$ mice and on day 2 post RWN infection. **(A)** Expression of indicated cytokines, IFNs, and ISGs in naïve $MAVS^{KO}$ and WT mice. Expression of GAPDH was used to normalize the samples. Shown are the combined data of 2 experiments using 3–4 mice/genotype. Differences between $MAVS^{KO}$ and WT mice were not significant. **(B)** Expression of IL-1β, IL-6, and TNF-α mRNA RWN-infected $MAVS^{KO}$ and $MAVS^{WT}$ mice on day 2 post infection. **(C)** Expression of type I and type III IFNs mRNA in RWN-infected $MAVS^{KO}$ and $MAVS^{WT}$ mice on day 2 post infection. **(C)** Expression of representative ISGs in RWN-infected $MAVS^{KO}$ and $MAVS^{WT}$ mice on day 2 post infection. **(B-D)** mRNA was isolated from whole dLN cells of mice 48 hours after infection with 10^5 Pfu RWN/footpad and measured by qPCR. Shown is the expression over that of dLNs from naïve WT mice. Expression of GAPDH was used to normalize the samples. Shown are the combined data of 4 experiments using 8–12 mice/genotype **, $p < 0.005$; ***, $p < 0.0005$; Mann-Whitney test.
(TIF)

S8 Fig. Normal production of systemic type I IFN in the serum of RWN-infected $MAVS^{KO}$ mice. Serially diluted serum samples from day 1 of RWN-infected mice were used to protect L929 cells from the cytopathic effects (CPE) of vesicular stomatitis virus (VSV) *in vitro*. Samples from mice immunized with OVA + LPS were used as positive controls. All samples were compared to samples treated with increasing doses of recombinant IFN-α2 as standards. Shown are the combined data from two experiments. Each dot represents one mouse. n. s., not significant; Mann-Whitney test.
(TIF)

S9 Fig. Neutralization index for sera of RWN-infected $MAVS^{KO}$ mice based on the titers of DIII-specific antibodies. **(A)** Virus neutralization with sera from $MAVS^{KO}$ and $MAVS^{WT}$ mice. **(B)** Neutralization index for the same mice based on the DIII-specific IgM and IgG titers (Dilution factor divided by the total amount of DIII-specific IgM and IgG). Each dot represents one mouse, the line is the median. Shown are the combined data of two experiments. **, $p < 0.005$; ****, $p < 0.00005$; Mann-Whitney test.
(TIF)

Acknowledgments

We thank Drs. Deepta Bhattacharya, Michael Kuhns, and Janko Nikolich-Žugich for critical reagents, technical help, and overall comments and suggestions.

Author Contributions

Conceptualization: Dominik Schenten.

Data curation: Marvin O'Ketch, Spencer Williams.

Formal analysis: Marvin O'Ketch, Spencer Williams, Dominik Schenten.

Funding acquisition: Dominik Schenten.

Investigation: Marvin O'Ketch, Spencer Williams, Cameron Larson, Brenna Hall.

Methodology: Marvin O'Ketch, Dominik Schenten.

Resources: Jennifer L. Uhrlaub, Rachel Wong, Neha R. Deshpande.

Supervision: Dominik Schenten.

Visualization: Marvin O'Ketch, Dominik Schenten.

Writing – original draft: Dominik Schenten.

References

1. Schenten D, Medzhitov R. The control of adaptive immune responses by the innate immune system. Adv Immunol. 2011; 109:87–124. https://doi.org/10.1016/B978-0-12-387664-5.00003-0 PMID: 21569913
2. Iwasaki A, Medzhitov R. Control of adaptive immunity by the innate immune system. Nat Immunol. 2015; 16:343–353. https://doi.org/10.1038/ni.3123 PMID: 25789684
3. Moyer TJ, Zmolek AC, Irvine DJ. Beyond antigens and adjuvants: Formulating future vaccines. Journal of Clinical Investigation. 2016. https://doi.org/10.1172/JCI81083 PMID: 26928033
4. Georg P, Sander LE. Innate sensors that regulate vaccine responses. Current Opinion in Immunology. 2019. https://doi.org/10.1016/j.coi.2019.02.006 PMID: 30978666
5. Pulendran B, Oh JZ, Nakaya HI, Ravindran R, Kazmin DA. Immunity to viruses: Learning from successful human vaccines. Immunol Rev. 2013. https://doi.org/10.1111/imr.12099 PMID: 23947360
6. Querec T, Bennouna S, Alkan S, Laouar Y, Gorden K, Flavell R, et al. Yellow fever vaccine YF-17D activates multiple dendritic cell subsets via TLR2, 7, 8, and 9 to stimulate polyvalent immunity. J Exp Med. 2006. https://doi.org/10.1084/jem.20051720 PMID: 16461338
7. Querec TD, Akondy RS, Lee EK, Cao W, Nakaya HI, Teuwen D, et al. Systems biology approach predicts immunogenicity of the yellow fever vaccine in humans. Nat Immunol. 2009. https://doi.org/10.1038/ni.1688 PMID: 19029902
8. Sander LE, Davis MJ, Boekschoten M V, Amsen D, Dascher CC, Ryffel B, et al. Detection of prokaryotic mRNA signifies microbial viability and promotes immunity. Nature. 2011; 474:385–389. https://doi.org/10.1038/nature10072 PMID: 21602824
9. Barbet G, Sander LE, Geswell M, Leonardi I, Cerutti A, Iliev I, et al. Sensing Microbial Viability through Bacterial RNA Augments T Follicular Helper Cell and Antibody Responses. Immunity. 2018. https://doi.org/10.1016/j.immuni.2018.02.015 PMID: 29548673
10. Ugolini M, Gerhard J, Burkert S, Jensen KJ, Georg P, Ebner F, et al. Recognition of microbial viability via TLR8 drives T FH cell differentiation and vaccine responses. Nat Immunol. 2018. https://doi.org/10.1038/s41590-018-0068-4 PMID: 29556002
11. Pulendran B, Ahmed R. Immunological mechanisms of vaccination. Nat Immunol. 2011; 12:509–517. Available: http://www.ncbi.nlm.nih.gov/pubmed/21739679 https://doi.org/10.1038/ni.2039 PMID: 21739679
12. Burchill MA, Tamburini BA, Pennock ND, White JT, Kurche JS, Kedl RM. T cell vaccinology: exploring the known unknowns. Vaccine. 2013; 31:297–305. https://doi.org/10.1016/j.vaccine.2012.10.096 PMID: 23137843
13. Coffman RL, Sher A, Seder RA. Vaccine adjuvants: Putting innate immunity to work. Immunity. 2010. https://doi.org/10.1016/j.immuni.2010.10.002 PMID: 21029960
14. Dixit E, Kagan JC. Intracellular pathogen detection by RIG-I-like receptors. Adv Immunol. 2013; 117:99–125. https://doi.org/10.1016/B978-0-12-410524-9.00004-9 PMID: 23611287
15. Chan YK, Gack MU. RIG-I-like receptor regulation in virus infection and immunity. Curr Opin Virol. 2015; 12:7–14. https://doi.org/10.1016/j.coviro.2015.01.004 PMID: 25644461
16. Bruns AM, Horvath CM. Activation of RIG-I-like receptor signal transduction. Crit Rev Biochem Mol Biol. 2012; 47:194–206. https://doi.org/10.3109/10409238.2011.630974 PMID: 22066529

17. Suthar MS, Ma DY, Thomas S, Lund JM, Zhang N, Daffis S, et al. IPS-1 is essential for the control of West Nile virus infection and immunity. PLoS Pathog. 2010; 6:e1000757. https://doi.org/10.1371/journal.ppat.1000757 PMID: 20140199

18. Da Costa A, Garza E, Graham JB, Swarts JL, Soerens AG, Gale M, et al. Extrinsic MAVS signaling is critical for Treg maintenance of Foxp3 expression following acute flavivirus infection. Sci Rep. 2017; 7:40720. https://doi.org/10.1038/srep40720 PMID: 28094802

19. Luo H, Winkelmann E, Xie G, Fang R, Peng BH, Li L, et al. MAVS Is Essential for Primary CD4+ T Cell Immunity but Not for Recall T Cell Responses following an Attenuated West Nile Virus Infection. J Virol. 2017;91. https://doi.org/10.1128/JVI.02097-16 PMID: 28077630

20. Widman DG, Ishikawa T, Winkelmann ER, Infante E, Bourne N, Mason PW. RepliVAX WN, a single-cycle flavivirus vaccine to prevent West Nile disease, elicits durable protective immunity in hamsters. Vaccine. 2009; 27:5550–5553. https://doi.org/10.1016/j.vaccine.2009.07.016 PMID: 19635608

21. Widman DG, Ishikawa T, Fayzulin R, Bourne N, Mason PW. Construction and characterization of a second-generation pseudoinfectious West Nile virus vaccine propagated using a new cultivation system. Vaccine. 2008; 26:2762–2771. https://doi.org/10.1016/j.vaccine.2008.03.009 PMID: 18423946

22. Nelson MH, Winkelmann E, Ma Y, Xia J, Mason PW, Bourne N, et al. Immunogenicity of RepliVAX WN, a novel single-cycle West Nile virus vaccine. Vaccine. 2010. https://doi.org/10.1016/j.vaccine.2010.10.069 PMID: 21055493

23. Diamond MS, Sitati EM, Friend LD, Higgs S, Shrestha B, Engle M. A Critical Role for Induced IgM in the Protection against West Nile Virus Infection. J Exp Med. 2003. https://doi.org/10.1084/jem.20031223 PMID: 14662909

24. Sitati EM, Diamond MS. CD4+ T-Cell Responses Are Required for Clearance of West Nile Virus from the Central Nervous System. J Virol. 2006. https://doi.org/10.1128/JVI.01650-06 PMID: 17035323

25. Franz KM, Neidermyer WJ, Tan YJ, Whelan SPJ, Kagan JC. STING-dependent translation inhibition restricts RNA virus replication. Proc Natl Acad Sci U S A. 2018; 115:E2058–E2067. https://doi.org/10.1073/pnas.1716937115 PMID: 29440426

26. Steiner LA, Eisen HN. Sequential changes in the relative affinity of antibodies synthesized during the immune response. J Exp Med. 1967. https://doi.org/10.1084/jem.126.6.1161 PMID: 4168368

27. Eisen HN, Siskind GW. Variations in Affinities of Antibodies during the Immune Response. Biochemistry. 1964; 3:996–1008. Available: http://www.ncbi.nlm.nih.gov/pubmed/14214095 https://doi.org/10.1021/bi00895a027 PMID: 14214095

28. Victora GD, Schwickert TA, Fooksman DR, Kamphorst AO, Meyer-Hermann M, Dustin ML, et al. Germinal center dynamics revealed by multiphoton microscopy with a photoactivatable fluorescent reporter. Cell. 2010. https://doi.org/10.1016/j.cell.2010.10.032 PMID: 21074050

29. Schenten D, Nish SA, Lee HK, Pasman L, Brodsky I, Yu S, Yordi B, Medzhitov R. Toll-like receptor-induced IL-1 releases naïve CD4+ T cells from regulatory T cell-mediated suppression in vivo. Immunity. 2014; 40:78–90. https://doi.org/10.1016/j.immuni.2013.10.023 PMID: 24439266

30. Nish SA, Schenten D, Wunderlich FT, Pope SD, Gao Y, Hoshi N, Yu S, Lee HK, Pasman L, Brodsky I, Yordy B, Zhao H, Brünning J, Medzhitov R. T cell-intrinsic role of IL-6 signaling in primary and memory responses. Elife (Cambridge). 2014; 3:e01949. https://doi.org/10.7554/eLife.01949 PMID: 24842874

31. Beasley DW, Barrett AD. Identification of neutralizing epitopes within structural domain III of the West Nile virus envelope protein. J Virol. 2002; 76:13097–13100. Available: http://www.ncbi.nlm.nih.gov/pubmed/12438639 https://doi.org/10.1128/jvi.76.24.13097-13100.2002 PMID: 12438639

32. Oliphant T, Engle M, Nybakken GE, Doane C, Johnson S, Huang L, et al. Development of a humanized monoclonal antibody with therapeutic potential against West Nile virus. Nat Med. 2005; 11:522–530. https://doi.org/10.1038/nm1240 PMID: 15852016

33. Nybakken GE, Oliphant T, Johnson S, Burke S, Diamond MS, Fremont DH. Structural basis of West Nile virus neutralization by a therapeutic antibody. Nature. 2005; 437:764–769. https://doi.org/10.1038/nature03956 PMID: 16193056

34. Purtha WE, Tedder TF, Johnson S, Bhattacharya D, Diamond MS. Memory B cells, but not long-lived plasma cells, possess antigen specificities for viral escape mutants. J Exp Med. 2011; 208:2599–2606. https://doi.org/10.1084/jem.20110740 PMID: 22162833

35. Diamond MS, Shrestha B, Marri A, Mahan D, Engle M. B Cells and Antibody Play Critical Roles in the Immediate Defense of Disseminated Infection by West Nile Encephalitis Virus. J Virol. 2003. https://doi.org/10.1128/jvi.77.4.2578-2586.2003 PMID: 12551996

36. Austin SK, Dowd KA. B cell response and mechanisms of antibody protection to West Nile virus. Viruses. 2014; 6:1015–1036. https://doi.org/10.3390/v6031015 PMID: 24594676

37. Zhao J, Vijay R, Zhao J, Gale M Jr., Diamond MS, Perlman S. MAVS Expressed by Hematopoietic Cells Is Critical for Control of West Nile Virus Infection and Pathogenesis. J Virol. 2016; 90:7098–7108. https://doi.org/10.1128/JVI.00707-16 PMID: 27226371

38. Sitati E, McCandless EE, Klein RS, Diamond MS. CD40-CD40 Ligand Interactions Promote Trafficking of CD8+ T Cells into the Brain and Protection against West Nile Virus Encephalitis. J Virol. 2007. https://doi.org/10.1128/JVI.00941-07 PMID: 17626103

39. Xia J, Winkelmann ER, Gorder SR, Mason PW, Milligan GN. TLR3- and MyD88-Dependent Signaling Differentially Influences the Development of West Nile Virus-Specific B Cell Responses in Mice following Immunization with RepliVAX WN, a Single-Cycle Flavivirus Vaccine Candidate. J Virol. 2013. https://doi.org/10.1128/JVI.01469-13 PMID: 23986602

40. Diamond MS, Pierson TC, Fremont DH. The structural immunology of antibody protection against West Nile virus. Immunological Reviews. 2008. https://doi.org/10.1111/j.1600-065X.2008.00676.x PMID: 18837784

41. Crill WD, Trainor NB, Chang GJJ. A detailed mutagenesis study of flavivirus cross-reactive epitopes using west Nile virus-like particles. J Gen Virol. 2007. https://doi.org/10.1099/vir.0.82640-0 PMID: 17374760

42. Crill WD, Chang G-JJ. Localization and Characterization of Flavivirus Envelope Glycoprotein Cross-Reactive Epitopes. J Virol. 2004. https://doi.org/10.1128/JVI.78.24.13975-13986.2004 PMID: 15564505

43. Choi KS, Nah JJ, Ko YJ, Kim YJ, Joo YS. The DE loop of the domain III of the envelope protein appears to be associated with West Nile virus neutralization. Virus Res. 2007. https://doi.org/10.1016/j.virusres.2006.09.002 PMID: 17027114

44. Sánchez MD, Pierson TC, McAllister D, Hanna SL, Puffer BA, Valentine LE, et al. Characterization of neutralizing antibodies to West Nile virus. Virology. 2005. https://doi.org/10.1016/j.virol.2005.02.020 PMID: 15866072

45. Pierson TC, Xu Q, Nelson S, Oliphant T, Nybakken GE, Fremont DH, et al. The stoichiometry of antibody-mediated neutralization and enhancement of West Nile virus infection. Cell Host Microbe. 2007; 1:135–145. https://doi.org/10.1016/j.chom.2007.03.002 PMID: 18005691

46. Peiris JSM, Porterfield JS. Antibody-mediated enhancement of Flavivirus replication in macrophage-Like cell lines [15]. Nature. 1979. https://doi.org/10.1038/282509a0 PMID: 503230

47. Peiris JSM, Gordon S, Unkeless JC, Porterfield JS. Monoclonal anti-Fc receptor IgG blocks antibody enhancement of viral replication in macrophages. Nature. 1981. https://doi.org/10.1038/289189a0 PMID: 7453820

48. Rodrigo WWSI, Jin X, Blackley SD, Rose RC, Schlesinger JJ. Differential Enhancement of Dengue Virus Immune Complex Infectivity Mediated by Signaling-Competent and Signaling-Incompetent Human FcγRIA (CD64) or FcγRIIA (CD32). J Virol. 2006. https://doi.org/10.1128/JVI.00792-06 PMID: 17005690

49. Bardina S V., Bunduc P, Tripathi S, Duehr J, Frere JJ, Brown JA, et al. Enhancement of Zika virus pathogenesis by preexisting antiflavivirus immunity. Science (80-). 2017. https://doi.org/10.1126/science.aal4365 PMID: 28360135

50. Halstead SB. Pathogenesis of dengue: Challenges to molecular biology. Science (80-). 1988. https://doi.org/10.1126/science.3277268 PMID: 3277268

51. Halstead SB, Shotwell H, Casals J. Studies on the pathogenesis of dengue infection in monkeys. I. clinical laboratory responses to primary infection. J Infect Dis. 1973. https://doi.org/10.1093/infdis/128.1.7 PMID: 4198027

52. Halstead SB. In vivo enhancement of dengue virus infection in rhesus monkeys by passively transferred antibody. J Infect Dis. 1979. https://doi.org/10.1093/infdis/140.4.527 PMID: 117061

53. Wang TT, Sewatanon J, Memoli MJ, Wrammert J, Bournazos S, Bhaumik SK, et al. IgG antibodies to dengue enhanced for FcγRIIIA binding determine disease severity. Science. 2017. https://doi.org/10.1126/science.aai8128 PMID: 28126818

54. Katzelnick LC, Gresh L, Halloran ME, Mercado JC, Kuan G, Gordon A, et al. Antibody-dependent enhancement of severe dengue disease in humans. Science (80-). 2017. https://doi.org/10.1126/science.aan6836 PMID: 29097492

55. Mehlhop E, Nelson S, Jost CA, Gorlatov S, Johnson S, Fremont DH, et al. Complement protein C1q reduces the stoichiometric threshold for antibody-mediated neutralization of West Nile virus. Cell Host Microbe. 2009; 6:381–391. https://doi.org/10.1016/j.chom.2009.09.003 PMID: 19837377

56. Yamanaka A, Kosugi S, Konishi E. Infection-Enhancing and -Neutralizing Activities of Mouse Monoclonal Antibodies against Dengue Type 2 and 4 Viruses Are Controlled by Complement Levels. J Virol. 2008. https://doi.org/10.1128/JVI.00992-07 PMID: 18003724

57. Mehlhop E, Ansarah-Sobrinho C, Johnson S, Engle M, Fremont DH, Pierson TCC, et al. Complement Protein C1q Inhibits Antibody-Dependent Enhancement of Flavivirus Infection in an IgG Subclass-Specific Manner. Cell Host Microbe. 2007. https://doi.org/10.1016/j.chom.2007.09.015 PMID: 18078693

58. Samuel MA, Diamond MS. Alpha/beta interferon protects against lethal West Nile virus infection by restricting cellular tropism and enhancing neuronal survival. J Virol. 2005; 79:13350–13361. https://doi.org/10.1128/JVI.79.21.13350-13361.2005 PMID: 16227257

59. Roe K, Giordano D, Young LB, Draves KE, Holder U, Suthar MS, et al. Dendritic cell-associated MAVS is required to control West Nile virus replication and ensuing humoral immune responses. PLoS One. 2019. https://doi.org/10.1371/journal.pone.0218928 PMID: 31242236

60. Braun D, Caramalho I, Demengeot J. IFN-alpha/beta enhances BCR-dependent B cell responses. Int Immunol. 2002; 14:411–419. Available: http://www.ncbi.nlm.nih.gov/pubmed/11934877 https://doi.org/10.1093/intimm/14.4.411 PMID: 11934877

61. Fink K, Lang KS, Manjarrez-Orduno N, Junt T, Senn BM, Holdener M, et al. Early type I interferon-mediated signals on B cells specifically enhance antiviral humoral responses. Eur J Immunol. 2006; 36:2094–2105. https://doi.org/10.1002/eji.200635993 PMID: 16810635

62. Coro ES, Chang WL, Baumgarth N. Type I IFN receptor signals directly stimulate local B cells early following influenza virus infection. J Immunol. 2006; 176:4343–4351. Available: http://www.ncbi.nlm.nih.gov/pubmed/16547272 https://doi.org/10.4049/jimmunol.176.7.4343 PMID: 16547272

63. Munoz-Jordan JL, Laurent-Rolle M, Ashour J, Martinez-Sobrido L, Ashok M, Lipkin WI, et al. Inhibition of Alpha/Beta Interferon Signaling by the NS4B Protein of Flaviviruses. J Virol. 2005. https://doi.org/10.1128/JVI.79.13.8004-8013.2005 PMID: 15956546

64. Suthar MS, Brassil MM, Blahnik G, Gale M. Infectious Clones of Novel Lineage 1 and Lineage 2 West Nile Virus Strains WNV-TX02 and WNV-Madagascar. J Virol. 2012. https://doi.org/10.1128/JVI.00401-12 PMID: 22573862

65. Welte T, Xie G, Wicker JA, Whitemanb MC, Li L, Rachamallu A, et al. Immune responses to an attenuated West Nile virus NS4B-P38G mutant strain. Vaccine. 2011. https://doi.org/10.1016/j.vaccine.2011.04.057 PMID: 21549792

66. Schenten D, Nish SA, Yu S, Yan X, Lee HK, Brodsky I, et al. Signaling through the adaptor molecule MyD88 in CD4+ T cells is required to overcome suppression by regulatory T cells. Immunity. 2014; 40:78–90. https://doi.org/10.1016/j.immuni.2013.10.023 PMID: 24439266

67. Ritvo P-GG, Churlaud G, Quiniou V, Florez L, Brimaud F, Fourcade G, et al. T_{fr} cells lack IL-2Rα but express decoy IL-1R2 and IL-1Ra and suppress the IL-1–dependent activation of T_{fh} cells. Sci Immunol. 2017. https://doi.org/10.1126/sciimmunol.aan0368 PMID: 28887367

68. Gitlin AD, Shulman Z, Nussenzweig MC. Clonal selection in the germinal centre by regulated proliferation and hypermutation. Nature. 2014; 509:637–640. https://doi.org/10.1038/nature13300 PMID: 24805232

69. Schwickert TA, Victora GD, Fooksman DR, Kamphorst AO, Mugnier MR, Gitlin AD, et al. A dynamic T cell-limited checkpoint regulates affinity-dependent B cell entry into the germinal center. J Exp Med. 2011. https://doi.org/10.1084/jem.20102477 PMID: 21576382

70. Kulkarni RR, Rasheed MAU, Bhaumik SK, Ranjan P, Cao W, Davis C, et al. Activation of the RIG-I Pathway during Influenza Vaccination Enhances the Germinal Center Reaction, Promotes T Follicular Helper Cell Induction, and Provides a Dose-Sparing Effect and Protective Immunity. J Virol. 2014. https://doi.org/10.1128/jvi.02273-14 PMID: 25253340

71. Sporri R, Reis e Sousa C. Inflammatory mediators are insufficient for full dendritic cell activation and promote expansion of CD4+ T cell populations lacking helper function. Nat Immunol. 2005; 6:163–170. https://doi.org/10.1038/ni1162 PMID: 15654341

72. Madsen L, Labrecque N, Engberg J, Dierich A, Svejgaard A, Benoist C, et al. Mice lacking all conventional MHC class II genes. Proc Natl Acad Sci U S A. 1999; 96:10338–10343. Available: http://www.ncbi.nlm.nih.gov/pubmed/10468609 https://doi.org/10.1073/pnas.96.18.10338 PMID: 10468609

73. Mombaerts P, Clarke AR, Rudnicki MA, Iacomini J, Itohara S, Lafaille JJ, et al. Mutations in T-cell antigen receptor genes alpha and beta block thymocyte development at different stages. Nature. 1992; 360:225–231. https://doi.org/10.1038/360225a0 PMID: 1359428

74. Kawai T, Takahashi K, Sato S, Coban C, Kumar H, Kato H, et al. IPS-1, an adaptor triggering RIG-I- and Mda5-mediated type I interferon induction. Nat Immunol. 2005. https://doi.org/10.1038/ni1243 PMID: 16127453

75. Uhrlaub JL, Brien JD, Widman DG, Mason PW, Nikolich-Zugich J. Repeated in vivo stimulation of T and B cell responses in old mice generates protective immunity against lethal West Nile virus encephalitis. J Immunol. 2011; 186:3882–3891. https://doi.org/10.4049/jimmunol.1002799 PMID: 21339368

76. Deshpande NR, Parrish HL, Kuhns MS. Self-recognition drives the preferential accumulation of promiscuous CD4(+) T-cells in aged mice. Elife (Cambridge). 2015; 4:e05949. https://doi.org/10.7554/eLife.05949 PMID: 26173205

77. Oliphant T, Nybakken GE, Austin SK, Xu Q, Bramson J, Loeb M, et al. Induction of epitope-specific neutralizing antibodies against West Nile virus. J Virol. 2007; 81:11828–11839. https://doi.org/10.1128/JVI.00643-07 PMID: 17715236

78. Fernandez E, Kose N, Edeling MA, Adhikari J, Sapparapu G, Lazarte SM, et al. Mouse and human monoclonal antibodies protect against infection by multiple genotypes of japanese encephalitis virus. MBio. 2018. https://doi.org/10.1128/mBio.00008-18 PMID: 29487230